Evaluation of State of Charge Estimation Algorithms for Battery Systems

Owen Brake, Justin Vuong, Frank Yan, Chris Samra, Hewitt McGaughey

***Abstract*— This study assesses various state-of-charge (SoC) estimation methods for lithium-ion batteries, focusing on a Samsung 30Q cell under dynamic loads. It compares four techniques: a naïve weighted sum, a weighted derivative method based on voltage curve slopes, an Extended Kalman Filter (EKF) for nonlinear dynamics, and a fuzzy logic system for managing sensor noise and uncertainties. Findings indicate that while the naïve and weighted derivative methods perform well under constant loads, they falter in variable conditions. Conversely, the EKF and fuzzy logic approaches excel, offering robust and reliable SoC estimates. This highlights the need for advanced SoC estimation methods to enhance battery management system functionality and safety in diverse applications, encouraging further development of hybrid strategies.**

***Index Terms*—Battery management systems, Electric vehicles, Lithium batteries, State estimation**

I. Introduction

Lithium-ion batteries serve as the powerhouse for numerous applications, from portable electronics to electric vehicles, emphasizing the critical need for accurate state of charge (SoC) estimation. The SoC, representing the remaining capacity of the battery, is pivotal for optimizing performance, prolonging battery life, and ensuring safe operation.

Voltage maps provide a snapshot of the battery's SoC by analyzing the voltage response during charge and discharge cycles. This method exploits the voltage dependence of the battery's electrochemical reactions, offering insights into its energy state. However, voltage-based estimation is susceptible to inaccuracies stemming from temperature variations, load fluctuations, and internal resistance changes. These limitations can compromise the reliability and robustness of its SoC estimation, particularly in dynamic operating conditions.

On the other hand, coulomb counting relies on integrating the current flowing in and out of the battery over time to track SoC changes. This method offers simplicity and low computational overhead, making it attractive for practical implementations. Nonetheless, coulomb counting suffers from cumulative errors, primarily due to current measurement inaccuracies, electrode polarization effects, and capacity degradation over the battery's lifespan. These factors undermine its precision, especially during prolonged usage or high levels of sensor noise.

Recognizing the inherent strengths and weaknesses of voltage maps and coulomb counting, the fusion of these methodologies aims to mitigate the shortcomings of individual methods.

In literature, a significant amount of work has gone into different fusion methods for SoC estimation. One study [1] compared a variety of different methods of SoC estimation. It concluded that, while Unscented Kalman Filters (UKFs) do provide slightly better SoC estimates, Extended Kalman Filters still have strong performance and "the estimation effect of the EKF algorithm is perfectly acceptable" [1].

Another journal that was considered investigated a method of fusing multiple voltage readings from the same pack [2]. This applies to the desired use case for this report but was never implemented due to scope issues.

One additional journal that was considered specifically detailed the implementation of an EKF for SoC estimation [3]. This journal gives an overview of specific EKF derivation and will be referenced in detail further in the report.

Finally, a journal regarding equivalent circuit modelling for lithium-ion battery pack SoC estimation was referenced to develop the model for the system used to test this report [4].

II. Background Knowledge

A. Lithium-Ion Battery Modelling

In battery management systems (BMS), accurate estimation of state of charge is paramount for ensuring optimal performance, longevity, and safety of lithium-ion batteries. One widely adopted approach involves employing mathematical models to simulate battery behavior and predict its dynamic response under varying operating conditions. Among these models, the 1RC (one resistor and one capacitor) equivalent circuit model stands out for its simplicity, versatility, and effectiveness in capturing the electrochemical dynamics of lithium-ion cells which is shown in Figure 1.

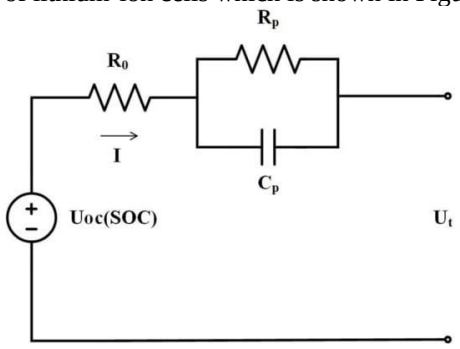

Figure 1. Circuit schematic of 1-RC battery model.

One crucial aspect addressed by the 1RC model is the discrepancy between the measured cell voltage and the relaxed cell voltage under no load conditions. When a battery is

discharged, its voltage sags from its no load state due to polarization effects, concentration gradients, and surface reactions. However, when the battery is left to rest without any external load, it tends to relax towards its intrinsic electrochemical equilibrium, leading to a different voltage level known as the relaxed cell voltage. By feeding the 1RC model into voltage map SoC estimations, a BMS can effectively account for the difference between measured cell voltage and relaxed cell voltage. This allows for more accurate tracking of the battery's true SoC when using voltage maps and facilitates proactive management strategies to optimize performance and prevent premature degradation.

B. *Samsung 30Q Battery Pack*

The Samsung 30Q is a Lithium Nickel Manganese Cobalt Oxide battery with a maximum charge voltage of 4.2 Volts, minimum discharging voltage of 2.5, and a capacity of 3000 milliampere-hours (mAh). To meet the energy requirements of larger-scale applications, such as electric vehicles or stationary energy storage systems, individual lithium-ion cells are often combined into battery packs through series and parallel connections. For this research study, a 20s6p (20 series cells each with 6 cells in parallel) configuration has been used to create a battery pack with a total capacity of 64800 Coulombs.

C. *Extended Kalman Filter for Sensor Fusion*

The Extended Kalman Filter (EKF) extends the basic Kalman Filter to handle nonlinear dynamics and non-Gaussian noise distributions. Despite its limitation of linear approximations, the EKF remains a versatile and widely used tool for state estimation in nonlinear systems, offering significant improvements over simpler techniques.

D. *Fuzzy Logic for Sensor Fusion*

Fuzzy logic offers a flexible and intuitive framework for handling uncertainty and imprecision in decision-making and control systems. The advantage of fuzzy logic fusion allows for nonlinear mapping between noisy sensor inputs and fused outputs, enabling the modeling of complex relationships and interactions between sensors in multisensory systems.

III. Method and Materials

A. *1RC Model System Identification*

Given the circuit model in Figure 1, the s-domain transfer function is derived as shown below.

$$V_o(s) = V_i(s) + I(s)(R_0 + \frac{1}{sC + \frac{1}{R_p}})$$

Given the transfer function step inputs are applied to attempt to fit the data to the derived model to extract bulk parameters R_0, R_p, C. The time domain solution for a step input to the transfer function is as follows.

$$V_o(t) = V_i(t) + I(R_0 + R_p\left(1 - e^{-\frac{t}{R_p C}}\right))$$

Applying an actual step current input yields the voltage response as shown in Figure 2, this response roughly matches the expected time domain solution, a sharp spike then exponential recovery.

At $t = 0$ of the step input the parameter R_0 is extracted, as $V_o - V_i = IR_0$. MATLAB is then used to fit a curve to the exponential recovery curve, this gets an approximate R_P, C. The values are found to be as follows:

$$R_0 = 3.1m\Omega$$
$$R_P = 1.5m\Omega$$
$$C = 9646.3F$$

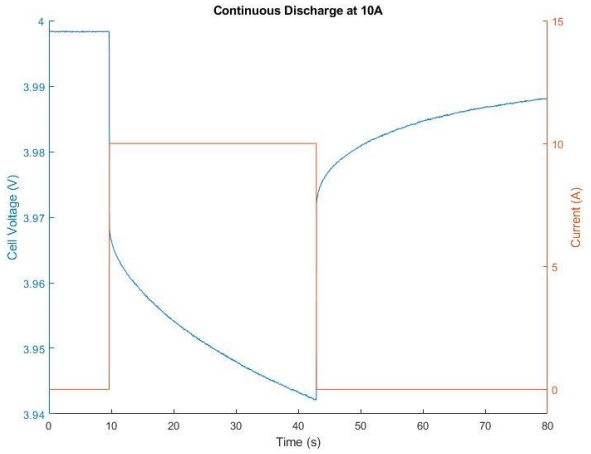

Figure 2. Open loop step current input and measured voltage response.

The derived resistance values nominally make sense, the DC internal resistance of the cells is measured to be ~$30m\Omega$ each, 6 in parallel is ~$5m\Omega$.

The derived capacitance value is very large and its actual value in Farads is somewhat meaningless, it is simply a proxy to emulate reactive behavior. It is very large due to the long time constant (~15 seconds) and very low resistance of R_P.

B. *System Emulation*

Given those derived parameters, an emulation model is developed. A time domain approximation for the 1-RC circuit model is found as follows.

$$V_{estimate}(t) = V_{measure}(t) + I(t)R_0 + V_C(t)$$
$$V_C(t) = \frac{1}{C}\int I(t) - \frac{1}{R_P}V_C(t)\,dt$$

C. *Model Results*

Implementing the system emulator in MATLAB and running it on the data yields a better estimated cell voltage. Figure 3 shows a correct cell voltage at a constant 10A discharge, and Figure 4 shows corrected cell voltage at a constant 30A discharge.

As it can be seen in the constant discharge data, the corrected cell voltage data has a significantly smaller drop than the raw data. Additionally, the adjusted cell voltage converges to the measured cell voltage at no load indicative of a correct model.

The adjusted cell voltage decreases quasi-linearly which also matches up with a constant discharge.

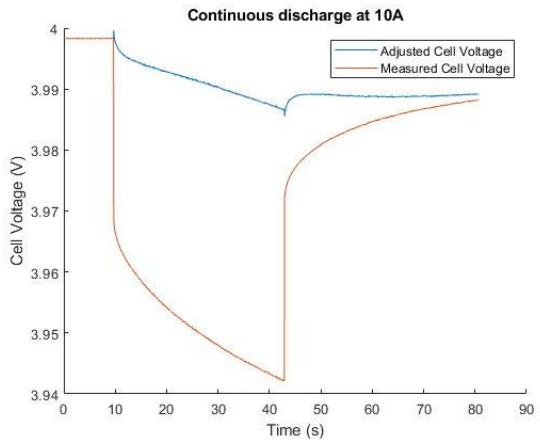

Figure 3. Corrected cell voltage at a 10A constant discharge using 1-RC model.

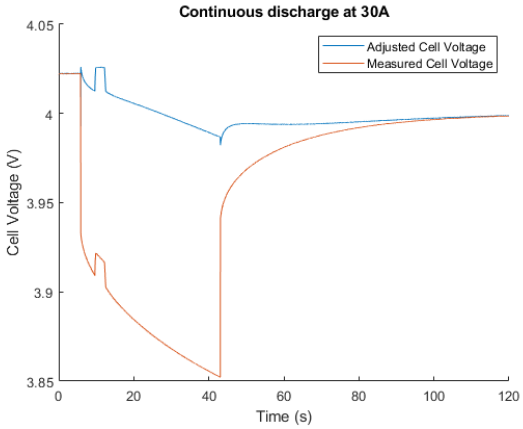

Figure 4. Corrected cell voltage at a 30A constant discharge using 1-RC model (there is a small blip in the data that is likely a firmware bug).

D. *Data collection*

The data collected for this report involves a custom BMS equipped with 20 16-bit analog-to-digital converters (ADC) that monitor cell voltages at 10Hz and a 24-bit ADC that measures current at 1000Hz. As seen in Figure 5, the battery was connected to a bidirectional power supply which drew varying loads from the battery pack.

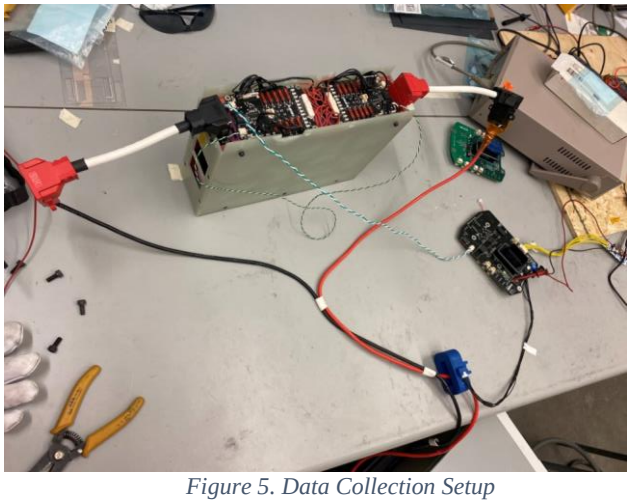

Figure 5. Data Collection Setup

To collect data for the discharge percentage to cell voltage curve, a low current draw was used to minimize the effects of internal resistance. Figure 6 serves as the basis for voltage based SoC estimation.

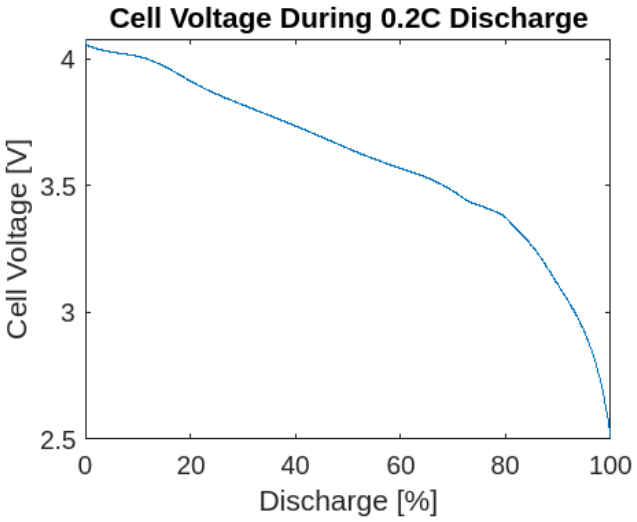

Figure 6. Experimental discharge percentage to voltage map.

E. *System Overview*

The block diagram of the planned fusion process for this system is shown in Figure 7 below.

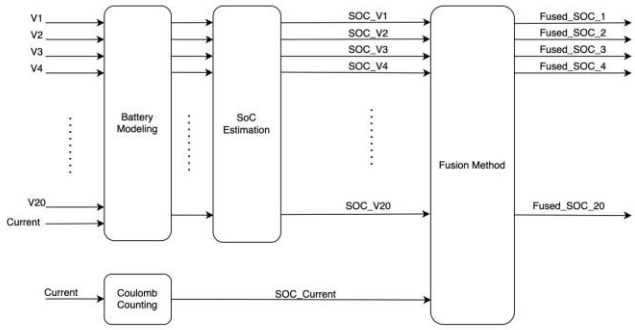

Figure 7. System block diagram.

The SoC for all 20 parallel groups of batteries is calculated using various methods explored in this report. The cell with the lowest SoC is then used as the SoC of the battery pack to ensure safe operation of the battery. Over-discharge of cells can lead to thermal runaway and catastrophic failure.

IV. RESULTS

Four approaches are used to estimate the SoC of the battery pack which are evaluated against each other to determine the most accurate method for dynamic load cases.

A. *Battery Model*

To validate the accuracy of the battery model in varying load cases, the measured and modelled battery voltages are plotted in Figure 8. These changes in measured cell voltage are indications of changing current loads which are corrected by the model leading to the steady drops in voltage over time

as was observed with the constant current based training data. Furthermore, long pauses of several minutes were introduced to the test data's varying load cases to demonstrate that the battery model converged to the relaxed cell voltage.

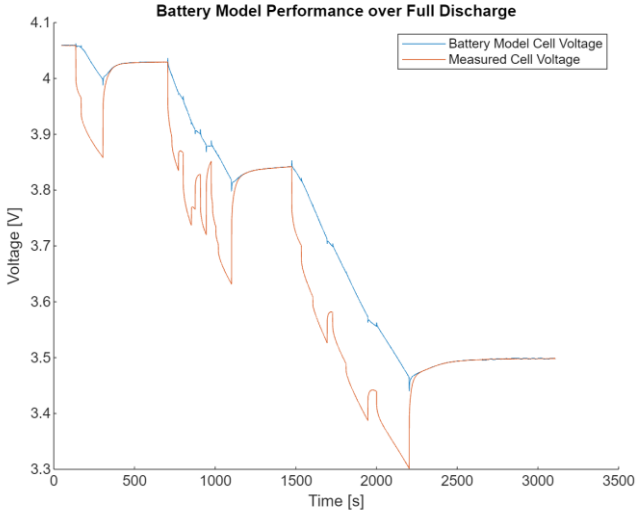

Figure 8. Results of the battery correction model over a full discharge cycle.

B. Naïve Approach

A simple solution to fusing the SoC values from the coulomb counting method and the voltage to SoC method is to use a weighted sum. The final fused state-of-charge for a cell is calculated as follows:

$$SOC_{fused} = \alpha * SOC_{voltage} + (1 - \alpha) * SOC_{current}$$

Where α is a weight from zero to one set by a piecewise function that modulates the relative importance of the voltage-based solution when compared to the coulomb counting approach. Figure 9 shows this piecewise weighting map:

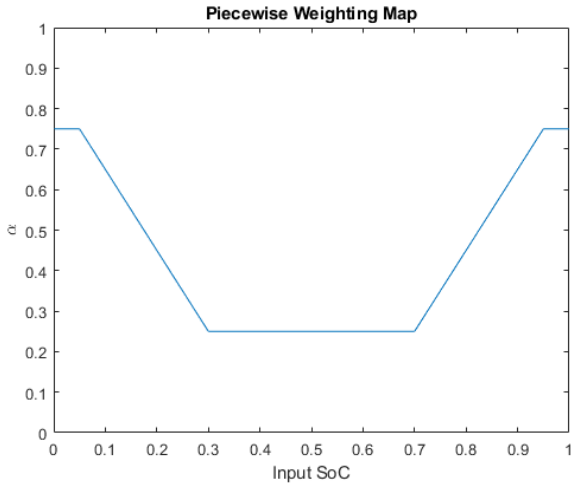

Figure 9. Piecewise function mapping input SoC estimates from the voltage map to weights for fusion.

The function in Figure 9 was constructed to emphasize how voltage SoC estimates need to be weighed heavier near the extreme ends to avoid operating the cell outside its voltage limits. Furthermore, the discharge to voltage map seen in Figure 6, does not demonstrate high rates of change in the linear region which means sensor noise on voltage measurements can greatly vary the estimated SoC. This is why a significant weight (70%) is assigned to coulomb counting from 30% to 70% as it does not face the same challenges. To avoid abrupt jumps in the estimated SoC, ramps are used in the piecewise function to smoothen the transition.

As an initial test for this method's performance, a constant 0.2C discharge is used for validation. Figure 10 shows the SoC estimates from only voltage estimates (blue), coulomb counting estimates (red), and the fused estimates (orange).

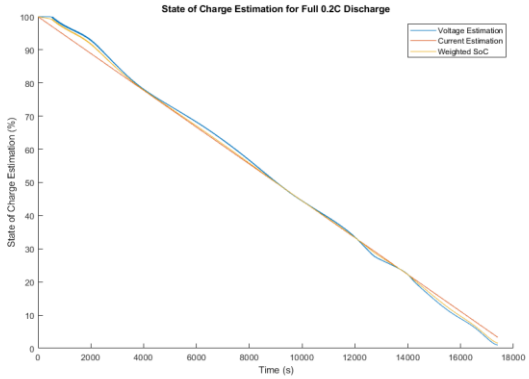

Figure 10. Naïve weighting for SoC estimations during a 0.2C discharge cycle.

Figure 11 shows current estimation as a perfect line which is expected for the constant current discharge case. The fused estimate performs well and is linear with some ripples at the beginning and end of the cycle, indicating that the voltage estimate takes precedence over the current estimate.

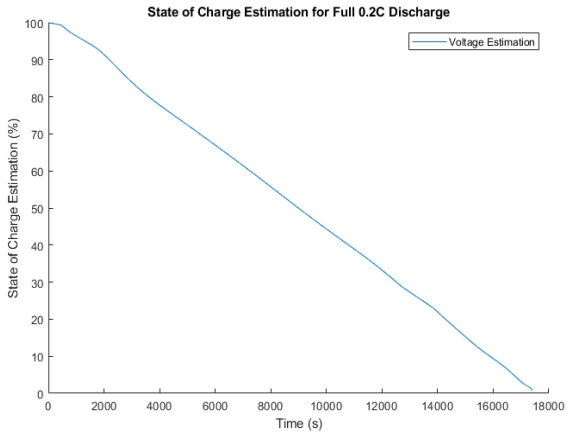

Figure 11. Naïve weighting for SoC estimations during a 0.2C discharge cycle, only showing voltage estimations.

C. Weighted Derivative Approach

To improve upon the naïve approach, the weights can be determined based on the slope of the SoC to voltage curve. In Figure 6, the cell voltage decreases slowly from 0% to 20% of the cycle, then decreases linearly from 20% to 60%, and from 80% to 100% it starts to drop faster near the end of the discharge cycle. This method uses the derivative from the linear region's slope to assign higher weights to the voltage based SoC estimation.

First, the discharge to cell voltage curve of Figure 6 is fit to

a 9th order polynomial which is the lowest order polynomial that captures the tails of the curve.

$$discharge\_percent\_to\_voltage = -1.0763 * 10^{-15}d^9 + 4.792 * 10^{-13}d^8 - 8.9621 * 10^{-11}d^7 + 9.0769 * 10^{-9}d^6 - 5.3899 * 10^{-7}d^5 + 1.889 * 10^{-5}d^4 - 3.7013 * 10^{-4}d^3 - 0.0035d^2 - 0.0172d + 4.0627$$

The linear region of this curve has a slope of -0.0088. A weighting function was experimentally found such that it weighed coulomb counting slightly higher than the voltage map estimates in the linear region. and gave significant importance to voltage maps around the extremities:

$voltage\_map\_weighting = 2(s - 0.0025)^{\frac{1}{3}} + 0.3$,

where s = |p+0.008| with p being the slope of the discharge to cell voltage curve.

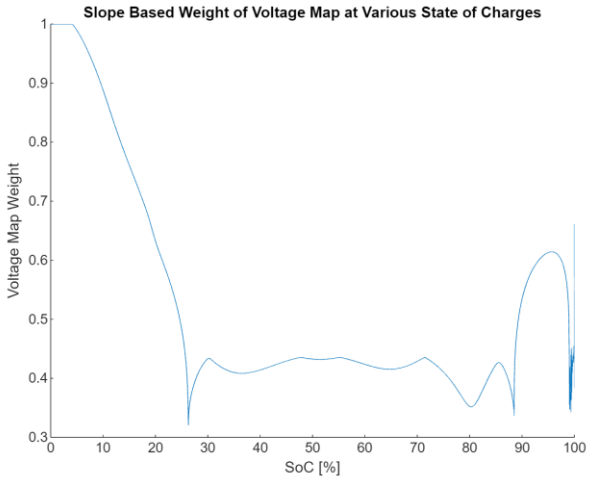

Figure 12. Slope-based weighting function on training data.

To generalize this model for the test data, the weights of this method are normalized and shown in Figure 12. This maps of the last estimated state of charge to a weight for the voltage SoC estimation. Like the naïve approach, the difference between 1 and the weight of the voltage approach is used as the weight for coulomb counting.

The performance of the weighted derivative approach on the training data is shown below in Figure 13.

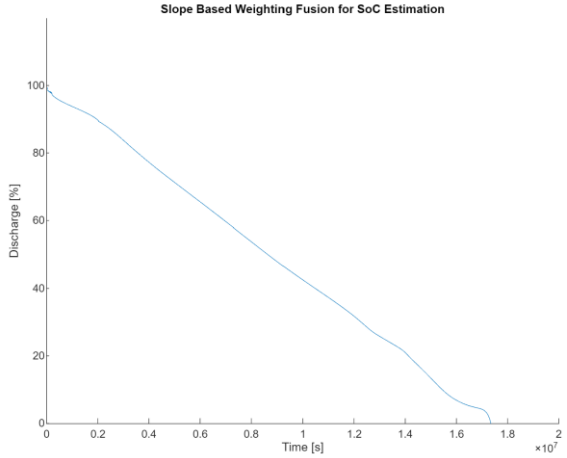

Figure 13. Slope-based fusion results on training data.

D. *Extended Kalman Filter*

Note that EKF work generally followed the same process defined in [3] and used some code snippets from previous EKF work by the authors of this paper [5].

Since a sensor noise estimation is needed for an EKF, a relaxed battery pack's voltage was measured to assess sensor noise. This yielded the following graph in Figure 14:

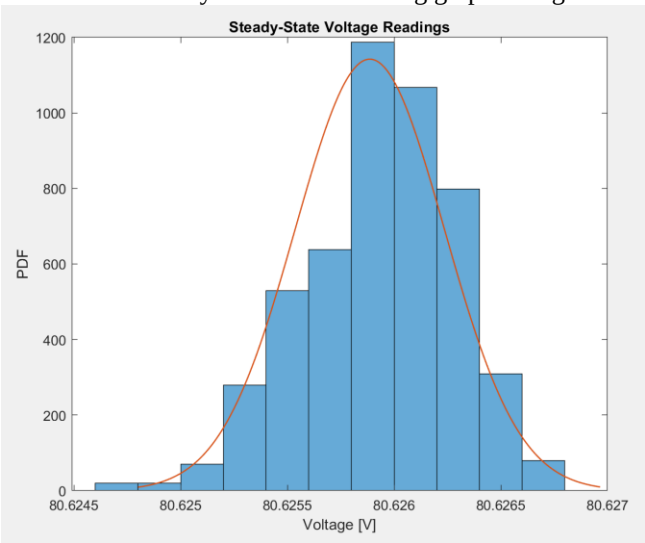

Figure 14. Histogram of 300 seconds of voltage readings at steady state, with a normal distribution fit to it.

The noise profile appears to be Gaussian and will be assumed to be for this report. Assuming zero-mean noise, this gives a standard deviation of σ = 0.000349.

As is commonly done in literature [3], the states were chosen for the EKF as follows:

$$x = \begin{bmatrix} SOC \\ V_{noload} \end{bmatrix}$$

Where SOC is the estimated decimal state-of-charge of the battery and V_{noload} is the estimated no-load voltage of each individual cell.

Similarly, the following process model is used:

$$x_k = f(x_{k-1}) = \begin{bmatrix} SOC_{k-1} + \frac{I\Delta t}{Q_{pack}} \\ soc\_to\_voltage(SOC_{k-1}) \end{bmatrix}$$

Where I is the current flowing into the pack and *soc_to_voltage* is the function, computed above, mapping an SoC value to an expected no-load relaxed cell voltage.

The following sensor model is used:

$$z_k = h(x_k) = \left[voltage\_uncorrected(V_{noload_{k-1}})\right]$$

Where we correct from the no-load voltage to the estimated "actual" voltage to compare it to the voltage reading for the pack.

Using the cell model, we have the following state transition matrix (note that it depends on the time step):

$$A = \begin{bmatrix} 1 & 0 \\ 0 & e^{\left(-\frac{\Delta t}{R_p C}\right)} \end{bmatrix}$$

Where R_p and C are cell properties defined in the system identification section.

The state observation matrix is calculated by numerically

differentiating the voltage estimation function around the previous SoC:

$$H = \left[\frac{d}{dSOC} soc\_to\_voltage \quad \frac{d}{dV} soc\_to\_voltage\right]$$

$$H = \left[\frac{d}{dSOC} soc\_to\_voltage \quad 1\right]$$

Finally, the following sensor covariance matrix is used, based on the standard deviation above.

$$R = [\sigma^2] = [1.2199 \times 10^{-7}]$$

Initially, the below covariance matrix was also used; note that it was tuned later to attempt to achieve better estimates. The current covariances are quite high as a test.

$$Q = \begin{bmatrix} 0.005 & 0 \\ 0 & 0.8 \end{bmatrix}$$

These are used in the full EKF to estimate SoC.

On the trial run with a constant 10A discharge for about 30 seconds, the following results in Figure 15 were obtained with an initial state estimate of $x_0 = \begin{bmatrix} 0.85 \\ 3.9 \end{bmatrix}$.

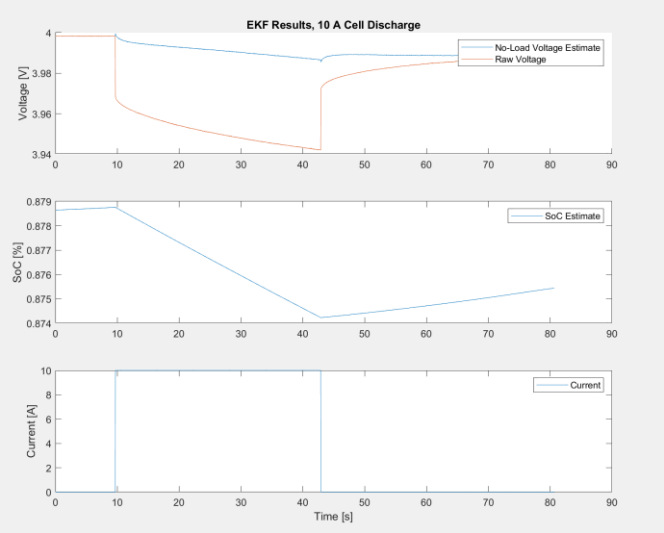

Figure 15. EKF test results for a constant 10 A discharge.

For the constant current training data, we have the following results in Figure 16:

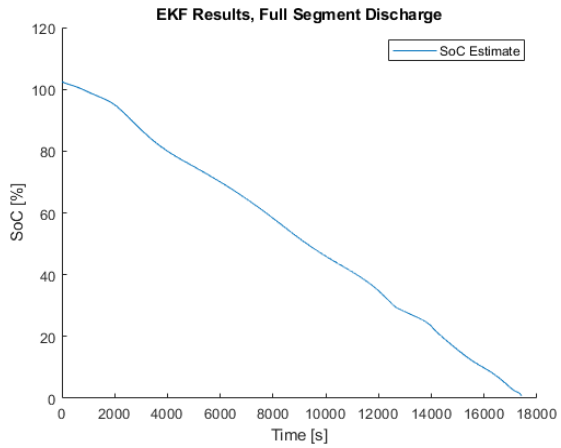

Figure 16. EKF results for the full segment discharge at constant current.

This graph is similarly quite reasonable and matches expectations for the full discharge. However, SoC initially starting above 100% is a slight concern, as are the slight dips in the curve due to possible voltage fluctuations.

E. Fuzzy Logic

One major issue the other methods have trouble with is dealing with nonlinearities. So far, the methods presented have made various assumptions about the operation of the battery but in practice a battery system has many nonlinearities which can be hard to model perfectly. Using fuzzy logic, nonlinearities and noisy measurements are less of an issue as the fuzzy logic system does not need to take these into account. Another advantage with the fuzzy logic approach is that a rule set can be built around the fusion of integrated current and voltage measurements.

The inputs for the fuzzy logic system are integrated current and the voltage of the cell after doing the adjustment mentioned in earlier sections. The output of the system is a state of charge estimate ranging from 0 to 100 percent. Three classes for the inputs and outputs are used: low, medium, and high. The membership functions and the ranges for each input are shown in Figure 17 and Figure 18.

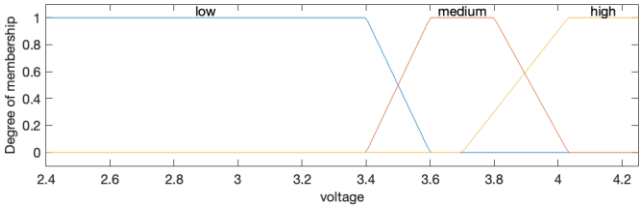

Figure 17. Fuzzy logic membership functions for the voltage measurement.

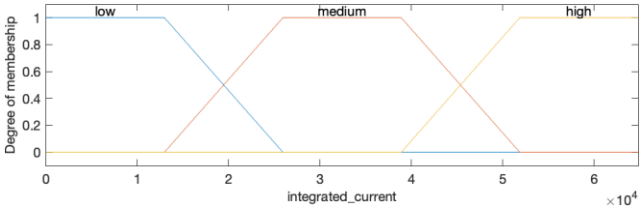

Figure 18. Fuzzy logic membership functions for the integrated current membership.

The voltage input ranges from 2.5 to 4.2V. 2.5V is the lowest possible voltage the segment is allowed to go to before damaging the segment which is why the minimum voltage is capped at 2.5V. Any voltage ranging from 2.5V to 3.4V is considered low with a membership of one. The maximum voltage of the segment is 4.2V, so any voltage from four volts to 4.2 volts is classified as high. Finally, any values between those bounds are considered as medium. As seen in Figure 17, the membership functions for the voltage input are all trapezoidal which is chosen for its simplicity.

For the integrated current input, the maximum charge is 64800 coulombs. To divide the membership functions, the ranges are divided by a percentage of the maximum charge. For example, a medium classification for integrated current should be around 40 to 60 percent of the maximum charge. Similar reasoning is used for the rest of the classifications where 0 to 20 percent is considered low and 80 to 100 percent is considered high.

The state of charge output the system needs to estimate is a continuous value. For this reason, a Sugeno fuzzy inference system is chosen to guarantee continuity for the output. As mentioned before the output can be put into one of three classes. The equations for each class are:

$$SOC_{low} = 30v - 0.00001c - 71.352$$
$$SOC_{medium} = 40v - 0.001c - 55.6$$
$$SOC_{high} = 60v - 0.0001c - 152$$

Where v is the voltage measurement and c is the integrated current measurement. To determine the weights, the training data of the constant current set is used to tune the weights so that the output of the system follows a linear trend.

The last piece of the fuzzy logic system is the rule set. The rule set of the fuzzy logic system is as follows:

1. If voltage is low and integrated_current is high then SoC is low
2. If voltage is medium or integrated_current is medium then SoC is medium
3. If voltage is high and integrated_current is low then SoC is high

Intuitively when the segment has not been discharged much (high state of charge), the integrated current measurement should be at a low value while the voltage measurement should be at a high value. When both measurements are in between, either one is suitable for estimating the state of charge which explains the structure of rule two using the "OR" operation.

Figure 19 presents the output of the fuzzy logic system on the same test data used in the previous methods – a constant current discharge cycle of 0.2C.

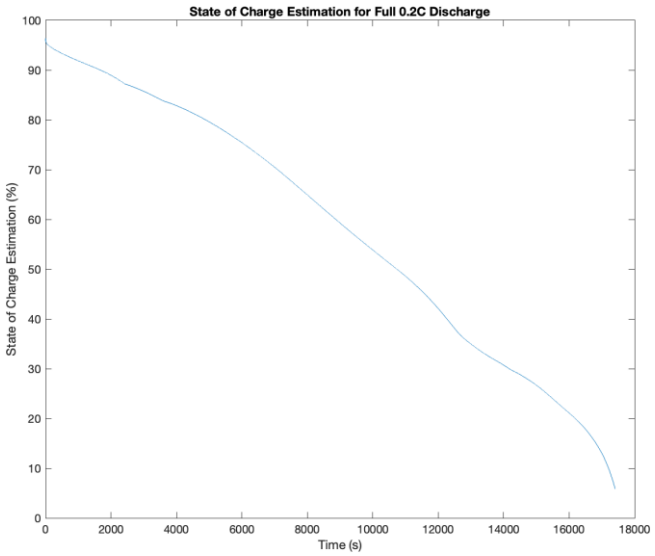

Figure 19. Fuzzy logic SoC estimation results on a constant-current 0.2C discharge cycle.

As expected, the estimation decreases over time and generally follows a linear trend. However, the output is not entirely linear. For example, from 12000 to 14000 seconds, there is a significant change in the slope. This is most likely due to the transition points of the fuzzy logic system when going from one output class to another. To improve upon this, additional tuning of the output function weights such as reducing the weight for the integrated current input can be done to smooth the transitions between the output classes.

F. Result Comparisons

To evaluate the performance of each of the methods, a test set of varying current is used. The current profile over time can be seen in Figure 20.

The evaluation process uses anchor points in the test data where no current is drawn, and the cells are given time to relax to their equilibrium states. The SoC to voltage map in Figure 6 is then used to get a ground truth estimate of the cell's state of charge as seen in Table 1. Finally, the time at which these states of charges are taken is compared against each fusion method.

Table 1. Ground truth values of state of charge for variable discharge cycle.

Settled Voltage (V)	Time (s)	State of Charge (%)
4.0291	652	93.5
3.8416	1457	72.1
3.4984	3062	32.6

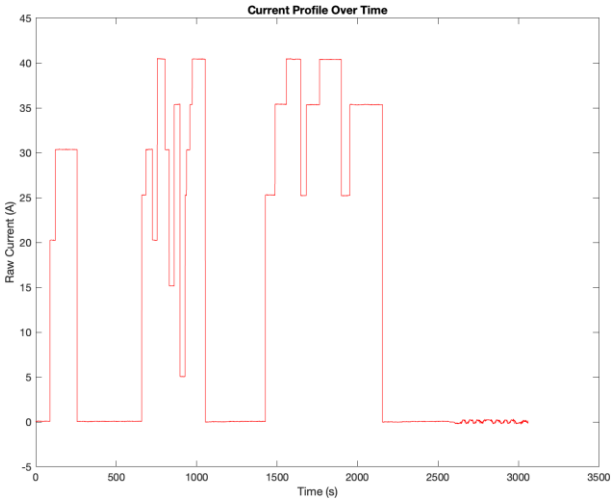

Figure 20. Graph of the discharge current over time for the full discharge evaluation cycle.

Figures 21 to 24 show plots of the state of charge curves for the naïve implementation, weighted slope method, EKF implementation, and fuzzy logic method on the test data respectively. The results for each are then summarized in Table 2.

1) *Naïve Approach Results*

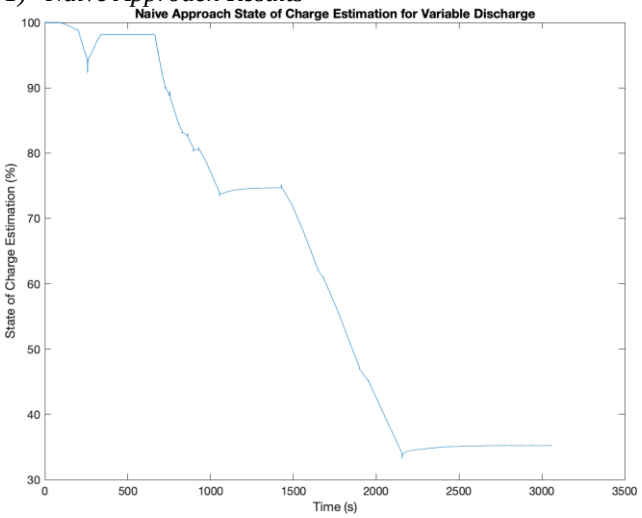

Figure 21. Naïve Implementation State of Charge Estimates on the Variable Load Test Set

Referencing Figure 21, the naïve approach plateaus at certain points and has spikes in its estimates. The change in state of charge estimates over time is not very smooth which can be attributed to the piecewise function used for the weighing function.

2) *Weighted Derivative Result*

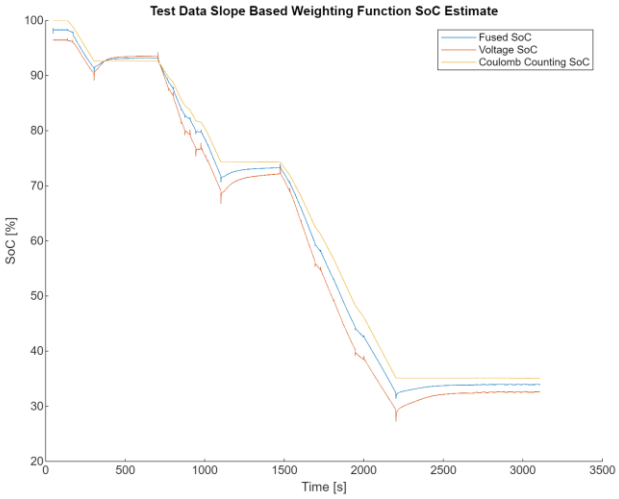

Figure 2222. Sloped Based Weighting Implementation State of Charge Estimates on the Variable Load Test Set

Like the naïve approach, the weighted derivative approach does not have a perfectly smooth and continuous SoC estimation which can be seen in Figure 22. This is attributed to the voltage SoC estimation having more significance than the coulomb counting approach. Generally, the coulomb counting approach estimates SoC higher than the voltage-based method. This helps to smooth out large changes in the voltage based SoC estimate curve. By fusing the estimates, this method tracks the ground truth values extremely well.

3) *EKF Results*

The initial state chosen for the EKF is a best rough guess:

$$x_0 = \begin{bmatrix} 0.99 \\ 4.05 \end{bmatrix}$$

The EKF results are shown in Figure 23. The EKF seems to generally underestimate the actual SoC, but when current is removed (at steady state), the SoC rises and approaches a quite good estimate, as expected.

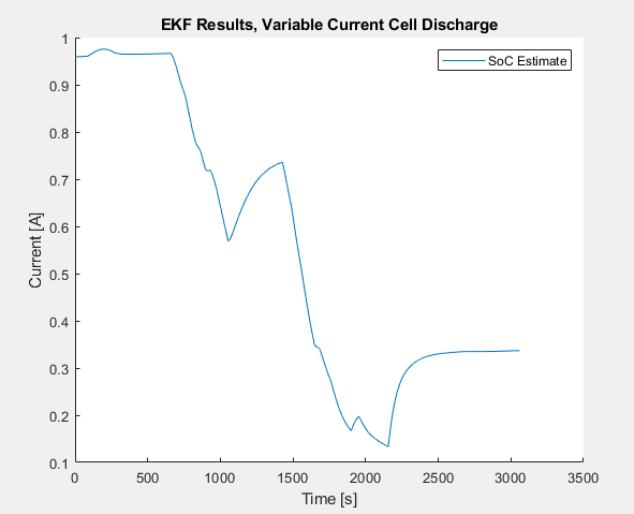

Figure 23. EKF State of Charge Estimates on the Variable Load Test Set

4) *Fuzzy Logic Results*

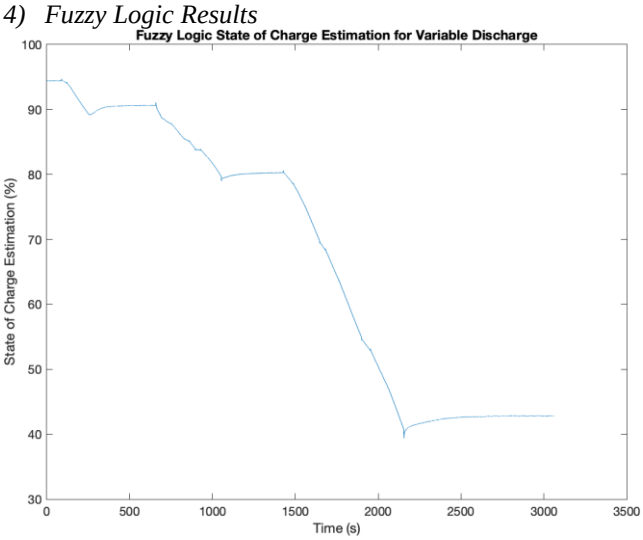

Figure 24. Fuzzy Logic State of Charge Estimates on the Variable Load Test Set

Like the naïve approach, the fuzzy logic estimates can be broken up into different regions from observing the change in state of charge estimates. This is most likely due to the different output membership functions the fuzzy logic system has where the transitions between the different classes are more visible in this case.

5) *Method Comparisons*

From Table 2, the weighted fusion method has the greatest number of values that are the closest to the ground truth values.

Table 22. Results Summary of each method

Method	SoC at 652 seconds	SoC at 1457 seconds	SoC at 3062 seconds
Ground Truth	93.5%	72.1%	32.6%
Naïve	98%	73%	35%
Weighted Fusion	93%	73%	33%
EKF	96.7%	68.7%	33.6%
Fuzzy Logic	91%	79.4%	42.8%

Both the EKF and naïve implementations overestimate the state of charge at the beginning but as the cycle continues, the estimates improve. The naïve implementation performs better than the EKF in the middle of the cycle but overestimates the state of charge at the end.

On the other hand, the fuzzy logic system seems to perform the worst overestimating all the state of charge values except for the first estimate by a significant margin.

Finally, an important note to be made is that these conclusions are made on only one validation set. To get more rigorous results additional testing should be done with different load currents and segments as one method may perform better than another. As a final note, each method can be additionally tuned and optimized to improve the performance by collecting more training data.

V. CONCLUSION AND RECOMMENDATIONS

This study evaluates four state-of-charge (SoC) estimation methods for lithium-ion batteries under dynamic conditions, using a Samsung 30Q cell. The methods assessed include a naïve weighted sum approach, a weighted derivative method based on the voltage-SoC curve, an Extended Kalman Filter (EKF), and fuzzy logic.

Each method exhibits distinct advantages and drawbacks. The naive method offers simplicity and reasonable accuracy, yet it's susceptible to noise and nonlinearities. The weighted approach demonstrates the best performance in test data, but further validation is required. While the EKF provides reasonable estimates and handles nonlinearities better, undesirable transients occur in estimation curves, suggesting a need for model accuracy enhancement and covariance matrix tuning. Despite its robustness to nonlinearities and noise, the fuzzy logic approach underperformed, necessitating additional tuning and data for evaluation.

For practical applications, the recommendation would be to use the EKF for the best accuracy if the only concern is to have extremely good readings at steady state. However, due to the poor transient performance of the EKF, using the weighted fusion method would be best if accurate SoC estimates are desired in all modes of operation.

REFERENCES

[1] J. He, S. Meng, and F. Yan, “A Comparative Study of SOC Estimation Based on Equivalent Circuit Models,” *Frontiers in Energy Research*, vol. 10, Jun. 2022, doi: https://doi.org/10.3389/fenrg.2022.914291.

[2] Z. He, “Efficient estimation method for State of Charge of multi-cell battery pack considering cell inconsistency,” *International Journal of Electrochemical Science*, p. ArticleID:220827, Aug. 2022, doi: https://doi.org/10.20964/2022.08.43.

[3] Z. Cui, W. Hu, G. Zhang, Z. Zhang, and Z. Chen, “An extended Kalman filter based SOC estimation method for Li-ion battery,” *Energy Reports*, vol. 8, pp. 81–87, Aug. 2022, doi: https://doi.org/10.1016/j.egyr.2022.02.116.

[4] R. Guo and W. Shen, “A Review of Equivalent Circuit Model Based Online State of Power Estimation for Lithium-Ion Batteries in Electric Vehicles,” *Vehicles*, vol. 4, no. 1, pp. 1–31, Dec. 2021, doi: https://doi.org/10.3390/vehicles4010001.

[5] H. McGaughey and O. Brake, “MTE 546 Lab 2 EKF,” University of Waterloo, Waterloo, Ontario, Canada, March 2024.